

RSC Advances



This is an *Accepted Manuscript*, which has been through the Royal Society of Chemistry peer review process and has been accepted for publication.

Accepted Manuscripts are published online shortly after acceptance, before technical editing, formatting and proof reading. Using this free service, authors can make their results available to the community, in citable form, before we publish the edited article. This *Accepted Manuscript* will be replaced by the edited, formatted and paginated article as soon as this is available.

You can find more information about *Accepted Manuscripts* in the [Information for Authors](#).

Please note that technical editing may introduce minor changes to the text and/or graphics, which may alter content. The journal's standard [Terms & Conditions](#) and the [Ethical guidelines](#) still apply. In no event shall the Royal Society of Chemistry be held responsible for any errors or omissions in this *Accepted Manuscript* or any consequences arising from the use of any information it contains.

Dielectric relaxation and Electro-optic response in nano- Ceria dispersed ferroelectric liquid crystal nanocomposites: Effect of structural deformation and lattice straining

Puja Goel^{*}, Manju Arora^{**}

^{*}Division of Agricultural Chemicals, Indian Agricultural Research Institute, New Delhi 110012, India.

^{**}CSIR- National Physical Laboratory, Dr. K.S. Krishnan Marg, New Delhi 110012, India.

* Email: pujagoel@gmail.com

The current investigations deal with the effect of CeO₂ nanoparticles (NPs) concentration on physical properties of Ferroelectric Liquid Crystal. Infrared transmission spectroscopy has been used to reveal the mechanism behind significant changes in dielectric behavior and electro-optic parameters of nanocomposites for the first time in correlation with structural deformation of functional group present in FLC and lattice straining induced by NPs. The temperature and frequency dependence of dielectric permittivity exhibits a gradual increase dielectric constant with CeO₂ NPs addition. The increase in saturated spontaneous polarization (P_s) and switching at a lower bias was also observed in these nanocomposites. IR transmission peaks pertaining to ν C=O and ν C-O stretching modes of FLC's ester (RCOOR') functional group showed shift in peak positions and appearance of new weak intensity C=O bonded chiral group vibrational mode at 1718 cm⁻¹ after Ceria dispersion. These variations are attributed to stress induced and coordinated bond formation between planar polar ester C=O group and Ce³⁺ ion through lone pairs of oxygen by CeO₂ NPs present in the interstitial sites of FLC's polar component. These structural distortions facilitate the easy polarizability of FLC molecules with enhancement in dielectric constant and P_s values. Additionally, loss profile demonstrates an increase in frequency and magnitude of ion linked relaxation and Goldstone Mode after ceria dispersion, whereas losses on their lower frequency side decrease.

Introduction

Ferroelectric Liquid Crystals (FLCs) have gained considerable research momentum from the past few decades as they render potential application in the field of flat panel displays, luminescent liquid crystal displays, spatial light modulators, optical storage, optical switching and electro-optic memory devices etc.¹⁻⁷ The incorporation of nanomaterials in FLCs has opened field widely for use in various novel multidisciplinary applications with marked enhancement in performance efficiency.

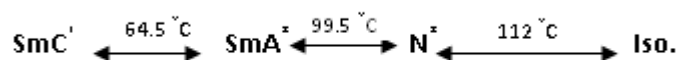
Earlier investigations have revealed that the interaction of NPs dispersed in FLCs nanocolloids play key role in determining the dielectric, optical and switching behavior which are requisite for their use in device applications. In addition to this, several new observations in dielectric and static memory effect, anomalous high and low frequency dielectric relaxations have been correlated with the type and size of doped NPs. The room temperature dielectric memory effect was reported for cobalt ferrite NPs (~ 9 nm) dispersed FLCs nanocomposites which become more pronounced as the temperature reaches smectic C* (SmC*) to smectic A (SmA) phase transition⁸. While in a mixture of FLC and Ni NPs⁹, a high frequency relaxation mode in conjunction with the collective dielectric mode is induced which persists even in the Sm A phase of the material. In addition to this, temperature dependent response time in FLC-Ni mixtures showed significant improvement owing to the combined effect of decreased rotational viscosity and slightly increased spontaneous polarisation in presence of Ni NPs. Dispersion of dye molecules in FLC has been found to change many physical properties of FLCs which depend upon dye molecular structure and its concentration.¹⁰In fullerene and FLC composite, illumination by the focused light of a halogen lamp alters complex permittivity in low frequency range due to formation of additional electron exchange channels between ions and electrode

through fullerene.¹¹ The doping of different size and concentration CdS nanorods in FLC and antiferroelectric liquid crystals (AFLC) have increased the spontaneous polarization, response time and photoluminescence.¹²⁻¹³ Among the metal oxide/rare earth oxide nanomaterials in FLCs studies, nano-Ceria (CeO_2) has imparted its optical properties to host FLC¹⁴. While Al_2O_3 NPs doping reduces ionic impurities effect in FLCs through their novel adsorption capability.¹⁵

Nano-ceria has drawn a great deal of attention owing to its high chemical stability, good dielectric strength, electronic tunability and optical properties. CeO_2 is a wide energy band gap semiconductor (e.g. 5.5 eV) which crystallizes in the fluorite crystal structure with space group *Fm3m* consisting of a face-centred cubic (f.c.c.) unit cell. Each cerium cation is coordinated by six nearest-neighbour oxygen anions to form CeO_6 octahedra, while each oxygen anion is shared by four nearest neighbour cerium cations¹⁶. Cerium (Ce) exists in Ce^{3+} and Ce^{4+} valence states. These oxidation states can auto regenerate and switchable due to nearly similar very low potential energy barrier to electron density distribution between 4f and 5d electronic states. The regeneration of Ce^{3+} ionic state at the surface of CeO_2 nanoparticles has been believed to be the origin of its core catalytic property.¹⁷⁻¹⁸ In the present study, we are mainly focusing on interaction of nano sized ceria particles with FLC (KCLFC 10s) in terms of role of functional groups and chiral centre present in FLC responsible for resulting dielectric relaxation and electro-optic parameters in composite formation with varied Ceria concentration. In this context, Infrared (IR) spectroscopy technique has been used to draw information about the molecular conformation in FLC, type of bonding of CeO_2 NPs with FLC and shift in peak positions with gain or loss in intensity. The variation in dielectric relaxation and spontaneous polarization has been tried to correlate with the deformation in ester functional group present adjacent to FLC chiral centre induced by CeO_2 NPs and presence of electronegative fluoride in biphenyl group.

Experimental

All the dielectric and electro-optic studies on FLC and nano-ceria dispersed composites were performed on electro-optic cells of thickness 4 μm which were fabricated using photolithography technique. Method of sample preparation has already been described in our previous report.¹⁴ For the fabrication of sample cells, glass plates with conducting ($\sim 30 \Omega/\square$) ITO coating were used. Electrodes of 4.5 mm \times 4.5 mm dimension were etched on these glass substrates after photoresist application followed by soft baking, mask alignment and UV exposure. Further, these patterned glass plates were spin coated with nylon polymer and hard baked at 180 $^{\circ}\text{C}$ for 20 minutes in order to achieve homogeneous alignment of FLC molecules. For the fabrication of nanocomposites, a suspension of Ceria NPs (Sigma Aldrich) was prepared by mixing 1g of CeO_2 NPs in 100 ml of Millipore water and 1 hr ultrasonication thereafter. Selective amounts of this suspension (i.e. 1, 3 and 5 μl of suspension) were admixed in a fix quantity of (3 mg) of FLC material. After this, mixtures were heated at about 115 $^{\circ}\text{C}$ and brought to isotropic phase, then mixed rigorously. This step was repeated thrice in order to ensure complete evaporation of water and homogenous dispersion of ceria nanoparticles into FLC matrix. Successively, pure and np- CeO_2 :FLC mixtures were introduced into the electro-optic cells at temperatures just above the Nematic*-Isotropic transition temperature (~ 112 $^{\circ}\text{C}$) of the FLC material used. The phase sequence of investigated FLC, i.e., KCFLC 10s (Kingston Chemicals Ltd.) is as follows:



where Cryst., SmC*, SmA, N*, and Iso., represent crystal, chiral smectic C, smectic A, chiral nematic, and isotropic phases, respectively.

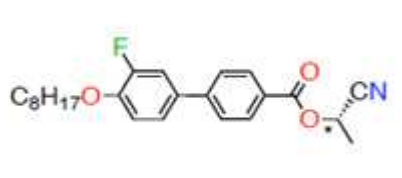
Effect of nano-ceria on the optical textures of KCFLC has already been reported¹⁴ and it was found that NPs are uniformly dispersed within the FLC and homogenous alignment could be retained up to 5 μl of ceria NPs dispersion. In order to identify the fundamental vibration of functional groups present in materials and to understand the structural deformation induced in FLC matrix on dispersing CeO₂ NPs, IR spectroscopy has been used. For this purpose, room temperature FTIR transmission spectra of CeO₂ NPs, FLC and np-CeO₂:FLC nanocomposites were recorded in 4000 – 500 cm^{-1} region on FTIR ALPHA T (Bruker make) spectrophotometer. In order to probe the collective and non-collective molecular processes in nanocomposites, frequency-temperature dependent dielectric measurements were performed by using a fully computer controlled and automated impedance analyzer (Wayne Kerr 6540A) in the frequency range of 20 Hz to 1 MHz. An Automatic Liquid Crystal Tester (ALCT-P) was used for analyzing the rotational viscosity, that is, η and spontaneous polarisation (Ps) in FLC-NPs dispersions.

Results and Discussion

Figure 1(a) shows the transmission bands observed in the IR spectrum of CeO₂ nanoparticles. The band observed at 1385 cm^{-1} is the characteristic vibration mode of CeO₂ while the absorption corresponding to Ce-O-C vibrational stretch is positioned at 837 cm^{-1} . The broad transmission band located 3430 cm^{-1} corresponds to the O–H stretching vibration of residual water and hydroxyl groups, whereas the absorption band at 1618 cm^{-1} is due to the scissor bending mode of associated water. Methylene (CH₂) of methyl group and CO₂ (atmospheric carbon dioxide) gives antisymmetric and symmetric stretching modes as very weak intensity peaks at 2925 and 2855 cm^{-1} and weak intensity bands at 2362 and 2344 cm^{-1} respectively. The very weak and weak

intensity bands observed at about 1167, 1050 cm^{-1} are observed due to traces of nitrate ion impurity (N-O), alkyl coordinated Ce^{4+} (R-O- Ce^{4+}) and R-O- Ce^{4+} / Ce^{3+} sample. These peaks arise from the impurity and coordination of Ce^{4+} / Ce^{3+} oxidation state with methyl group of alkyl chains used for the capping ceria NPs. The band at 804 cm^{-1} corresponds to C-H bending modes are observed as weak bands. The metal–oxygen ν Ce-O (of CeO_2) antisymmetric and symmetric stretching vibrational peaks¹⁹ as very strong transmissions at 669 and 559 cm^{-1} respectively.

IR spectra of pure FLC (Fig. (b)) gave valuable information about molecular conformations and fundamental vibration of functional groups present in FLC. In general, FLCs are mixtures of two or more organic compounds containing substituted biphenyl aromatic cores with aliphatic end chains and ester group adjacent to one or more chiral dopant. In this particular FLC, the smectic C host component is made up of difluoro-tera-phenyls, and the chiral dopant is a cyanohydrin ester as given below



As can be seen from Fig. 1 (b), vibrational modes pertaining to the functional groups of FLC substituted biphenyl core group and long alkyl chain with p-substitution through oxygen are present. IR activity of these modes has been attributed to polarization of all parallel modes averaged over long molecular axis. While, for C=O and CH₂ groups the maximum absorption arise from the polarization over perpendicular averaged molecular long axis. IR transmission spectrum in Figure 1(b) shows bands corresponding to $-\text{C}\equiv\text{N}$, $-\text{COO}$, $-\text{CH}_2$, $-\text{CH}_3$ and $-\text{C}=\text{C}-$

aromatic ring groups. The strong IR peaks observed in Fig. 1(b) are assigned as the fundamental modes arising from FLC cores at 1184, 1265, 1460, 1527, 1606 and 1732 cm^{-1} ; and from the alkyl chains at 2856, 2928 and 804 cm^{-1} respectively²⁰. The three very strong peaks at 2856, 2928 and 804 cm^{-1} are assigned as the symmetric, antisymmetric stretching and bending modes of CH_2 along the alkyl chains of the FLC molecules. The peak at 1732 cm^{-1} is attributed to $\text{C}=\text{O}$ stretching vibration mode of ester carbonyl group and the peaks at 1606 and 1527 cm^{-1} are obtained due to $\text{C}-\text{C}$ stretching modes of the FLC core. The combination mode of $\text{C}-\text{C}$ stretch and in-plane wagging vibration of $\text{C}-\text{H}$ of FLC core is observed at 1460 cm^{-1} . While the peaks at 1184 and 1265 cm^{-1} are associated to the symmetric and antisymmetric stretching vibration of $\text{C}-\text{O}-\text{C}$ group.

As shown in Fig. 1 (c-e) IR transmission spectra of np-CeO_2 :FLC exhibits the ordering of IR spectrum with the minor variation in peak positions of $\text{C}=\text{O}$ (ester carbonyl group) frequencies and the appearance of new weak intensity $\text{C}=\text{O}$ bonded chiral group vibrational mode at 1717~1718 cm^{-1} . In addition to this, intensity of $\text{C}-\text{O}$ stretching mode of ester (RCOOR') transmission peak is shifted from 1098 cm^{-1} to 1108 cm^{-1} in 1 μl ceria NPs dispersed FLC sample whereas it shifts to 1109 cm^{-1} after in 3 μl and 5 μl CeO_2 NPs dispersion. The ester group in FLCs is basically a planar linking group which entails lamellar packaging of molecules in a tilted smectic structure.²¹ The easy polarization of $\text{C}=\text{O}$ bond is induced by the delocalization of pi electrons over ester carbonyl group induced by adjacent chiral carbon and para bonded-biphenyl aromatic group with meta bonded strong electron donating fluoride. The shift in frequencies of these bands confirms the stress induced and coordinated bond formation between ester $\text{C}=\text{O}$ and Ce^{3+} ion through lone pairs of oxygen by CeO_2 NPs present in the interstitial sites of FLC component containing planar polar ester group of cored liquid crystal which facilitate the

easy polarizability of FLC, whereas alkyl chain bonded part is least affected by the addition of NPs because their peaks do not show major shift in their positions.

Spontaneous polarization, P_s , of FLCs is very important parameter for their applicability in electro-optic devices since their dynamic properties are governed by a change in the orientation of the spontaneous polarization and of the molecular director on the application of external electric fields. Switching response time, τ , which is another most important physical parameter, is inversely proportional to P_s ($\tau \propto 1/P_s \cdot E$).²² Therefore, a higher P_s is desirable for faster the switching of FLC. In order to see the effect of nano-ceria dispersion on FLC's spontaneous polarization (P_s), the P_s values were recorded at 30 °C temperature for pure and doped samples at different bias voltages and demonstrated in Figure 2 (a). Large and consistent increase in saturated P_s values can be noted with increasing the amount of nano-ceria concentration. In addition to this, switching takes place at 1.5 V bias in ceria dispersed samples whereas, in case of pure FLC, P_s could be noted only after applying 4.5 V bias. This indicates that ceria NPs are facilitating the switching of FLC molecules in external electric field and making it easier to obtain polarization at a bias as low as 1.5 V. It is well known that the spontaneous polarization in FLC is caused by electron delocalization over planar ester functional group bonded to adjacent chiral centre and fluoride bonded biphenyl aromatic core of the nearest neighbouring molecule through wide spread electron cloud. As explained in previous section, ceria is straining and forming coordination bond with the ester polar component linking group in FLC mixture. This facilitate the easy polarizability of FLC molecules and believed to be the main cause for increased value of spontaneous polarization and sensitivity towards electric field for ceria dispersed sample. The behavior of rotational viscosity (η) vs. applied bias voltages recorded at 30 °C in pure and ceria dispersed FLCs is shown in Fig. 2 (b). Bias dependent

behavior of viscosity follows the same profile of increase and decrease as that of pure FLC. Since, rotational viscosity coefficient of FLC describes the energy dissipation as a result of the director rotation, coordinated bond formation between guest and host molecules lead to steric hindrance with higher energy loss during the director reorientation process and resulted into a higher rotational viscosity for all the ceria dispersed analogues. Figure 2 (c) depicts the behavior of response time vs. applied bias voltages in pure and np-CeO₂:FLC composites. Higher P_s and lower rotational viscosity is desirable for faster obtaining faster response time since It is directly proportional to viscosity and inversely proportional to spontaneous polarization through the relation $\tau = \eta/P_s * E$. In our ceria dispersed FLC analogues, we have observed an increase in both P_s and η after ceria dispersion however the ratio of this enhancement (i.e. η/P_s) is such that, τ values do not show an increase beyond 4.5 V bias application.

To investigate the relaxation processes in fabricated nanocomposites, temperature and bias dependent dielectric spectroscopy was performed. Frequency variation of dielectric permittivity for pure FLC and np-CeO₂:FLC (1 and 5 μ l concentrations) is given in Figure 3(a)–(c) in temperature ranging from deep SmC* to Sm A* phase. As seen in Figure 3 (a), in undoped sample, the magnitude of ϵ' is very large in low frequency range (<1 KHz) which is mainly due to the Goldstone mode (phase fluctuations, few kHz range) contribution to the dielectric permittivity and considered as a usual behavior of FLC materials.⁸ Also, It can be seen that, as the temperature increases, Goldstone mode (GM) contribution to the permittivity in the SmC* phase decreases which lead to very low values of ϵ' near SmC* - SmA* transition region.

Further, to compare the effect of CeO₂ NPs addition on dielectric permittivity (ϵ') values, profiles of frequency dependent permittivity np-CeO₂: FLC nanocomposites are compared at 30 °C and shown in Fig. 4. After CeO₂ NPs addition, ϵ' increases on increasing the NPs concentration upto 5 μ l which suggests that the presence of NPs are enhancing the GM contribution to ϵ' .

In order to further elucidate the molecular dynamics in np-CeO₂:FLC systems, frequency dependent dielectric loss factor ($\tan \delta$) studies were performed. Figure 5 demonstrates the behavior of frequency vs. dielectric loss factor ($\tan \delta$) at different temperatures for pure and np-CeO₂:FLC nanocomposites (1 and 5 μl). As can be seen from Fig. 5(a), a low-frequency relaxation mode (~ 268 Hz) adjacent to typical GM is observed in the case of pure FLC (KCFLC 10 S) material. In general, collective and non-collective molecular processes in FLCs are represented by different dielectric relaxation modes such as Goldstone Mode (GM) and Soft Mode (SM). While GM is associated with the phase fluctuations in the azimuthal orientation of the molecular director, SM is due to fluctuations in the amplitude of the tilt angle.⁸ Additional low frequency relaxation mode, which has also been observed in previous studies conducted on KCFLC 7s and KCFLC 10s compounds, is attributed to the presence of ionic impurities.¹⁵ It can be noticed from Fig. 5a that this low frequency ionic impurity linked dielectric relaxation (ILDR) shifts towards higher frequencies on increasing the temperature and eventually merges with GM at ~ 46 °C in pure FLC.

Successively, the effect of Ceria NPs dispersion on the nature of collective, non collective and impurity linked (ILDR) dielectric relaxation could be seen in Fig. 5b-c. Low frequency relaxation peak appeared much closer to the GM peak and disappeared at ~ 36 °C temperature in ceria dispersed analogues. Further, a comparison of magnitude and frequency of relaxation of different modes with varying NPs concentration at 30 °C is depicted through Fig. 6. Incorporation of ceria NPs lead to an increase in the frequencies of both the relaxation modes. Although, the addition of variable concentration of NPs doesn't affect the frequency of GM, ILDR peak moves towards GM with increasing particle concentration and manifests as a single relaxation peak with np-CeO₂:FLC nanocomposites with 5 μl concentration. It can also be noted

that the GM peak magnitude also increases with Ceria NPs addition which yes again indicate the direct coordination of $\text{Ce}^{3+}/\text{Ce}^{4+}$ ions of ceria with FLC molecules that restrict the phase fluctuation mode leading to higher absorption of electric field energy. On contrary to this, losses below the GM mode or on the low frequency wing decreases in presence of Ceria NPs (Fig. 6 inset) and there is formation of crossover just on the onset of ILDR mode. The losses in ceria dispersed samples start increasing above the pure FLC's absorption peaks of ILDR and GM mode

Conclusions

Investigations on electro-optical and dielectric properties of Ceria NPs dispersed ferroelectric liquid crystal (FLC) have been made and the resulting changes have been understood in the light of structural deformation of the ester functional group which is a polar linking group present adjacent to FLC chiral center. Dielectric permittivity, P_s showed enhancement in their values and polarization switching takes place at a much lower bias voltage (1.5 V) in presence of Ceria NPs. This increase in dielectric permittivity and P_s has been attributed to the FLC lattice straining by the random distribution of CeO_2 NPs present in interstitial sites and structural deformation in polar component (ester group) by the coordination of Ce^{3+} ions as inferred from the FTIR transmittance spectra of FLC-Ceria sample. The shift in peak position of C=O and C-O stretching modes of ester (RCOOR') and appearance of new weak intensity peak of C=O bonded to FLC adjacent chiral group at 1718 cm^{-1} confirmed stress induced by the substitution of CeO_2 NPs in interstitial sites of FLC matrix and coordinated bond formation by lone pairs of carbonyl oxygen with CeO_2 NPs Ce^{4+} ions. Such type of linkages encourages the easy polarizability of FLC molecules. Additionally, loss profile ($\tan \delta$ vs Freq) exhibits an impurity related relaxation mode on the lower frequency side of GM in the Sm C* phase of the pure FLC material (KCFLC

10S) which shift towards high frequency side in FLC-Ceria NPs nanocomposites and manifests as a single relaxation peak at 5 μ l concentration.

Acknowledgment

The authors sincerely thank Director, IARI and Head, Agricultural Chemicals Division, IARI for continuous encouragement and interest in this work. Authors also wish to thank Sh. K.K. Somayajulu and Dr. Suresh for FTIR characterizations. One of the authors (P. Goel) is also thankful to DST, New Delhi for financial support under INSPIRE Faculty Scheme (IFA12-PH-38).

References

- ¹ P.G. De Gennes and J. Prost, *The Physics of Liquid Crystals*; Clarendon; Oxford Science Publications: Oxford, 1995.
- ² N.A.Clark and S.T. Lagerwall, *Appl. Phys. Lett.* 1980, **36**,899.
- ³ Ingo Dierking, *Polym. Chem.*, 2010.**1**. 1153.
- ⁴ P.J.Collings, *Liquid Crystals: Nature's Delicate Phase of Matter* (Princeton University Press, Princeton), (1990).
- ⁵ R. B. Meyer, L. Liebert, L. Strzelecki, and P. Keller, *J. Phys. Lett.*, 1975. **36**. 69.
- ⁶ W.Haase and S. Wrobel, *Relaxation Phenomena: Liquid Crystals, Magnetic Systems, Polymers, High-Tc Superconductors, Metallic Glasses*, Springer: Heidelberg, Germany, 2003
- ⁷ C. Weder, C. Sarwa, A. Montali, C. Bastiaansen and P. Smith, *Science*, 1998. **279**. 835
- ⁸ P Goel, G. Singh, R.P. Pant and A.M. Biradar, *Liquid Crystals*, 2012. **39 (8)**. 927.
- ⁹ P. Goel, P.L. Upadhyay and A.M. Biradar, *Liquid Crystals*, 2013. **40 (1)**. 45.
- ¹⁰ A.K. Srivastava, A.K. Misra, J.P. Shukla and R. Manohar, *Phys. Lett. A.*, 2008. **372(41)**. 6254.
- ¹¹ A.F.Shevchuk, D.A.Naiko, A.V. Koval'chuk, E.V. Basiuk (Golovataya-Dzhymbeeva), *Ukr. J. Phy.*, 2004. **49 (12 A)**.A21.
- ¹² P. Malik, A. Chaudhary, R. Mehra and K. K. Raina, *Adv. in Cond. Matter Phys.* 2012. Article **ID 853160**, 8 pages.
- ¹³ J.S. Roy, T.P. Majumder, R. Dabrowski, *Journal of Luminescence*. 2014. **148**. 330.
- ¹⁴ P. Goel, M. Arora and A. M. Biradar, *RSC Adv.*, 2014, **4**, 11351.
- ¹⁵ T. Joshi, J. Prakash, A.Kumar, J. Gangwar, A. K. Srivastava, S. Singh and A M Biradar, *J. Phys. D: Appl. Phys.* 2011.**44**.315404.
- ¹⁶ K. Schwarz, *Proc. Natl. Acad. Sci. U. S. A.*, 2006. **103**, 3497.
- ¹⁷ N. Shehata, K. Meehan, M. Hudait, N. Jain, *J Nanopart Res.*2012.**14**.1173.

¹⁸N. V. Skorodumova, R. Ahuja, S. I. Simak, I. A. Abrikosov, B. Johansson and B. I. Lundqvist, *Phys.Rev.B*, 2001. **64**. 115108.

¹⁹A. A. Athawale, M. S. Bapat and P. A. Desai, *J. Alloys. Compd.*, 2009. **484**.211.

²⁰J.G. Zhao, T. Yoshihara, H.W. Siesler and Y. Ozaki, *Phys. Rev. E*, 2001. **64**, 031704.

²¹Peter J. Collings, Michael Hird, *Introduction to Liquid Crystals: Chemistry and Physics*, Taylor and Francis, 1998.

²²P. Goel and A. M. Biradar, *Appl. Phys. Lett.*, 2012. **101**. 074109.

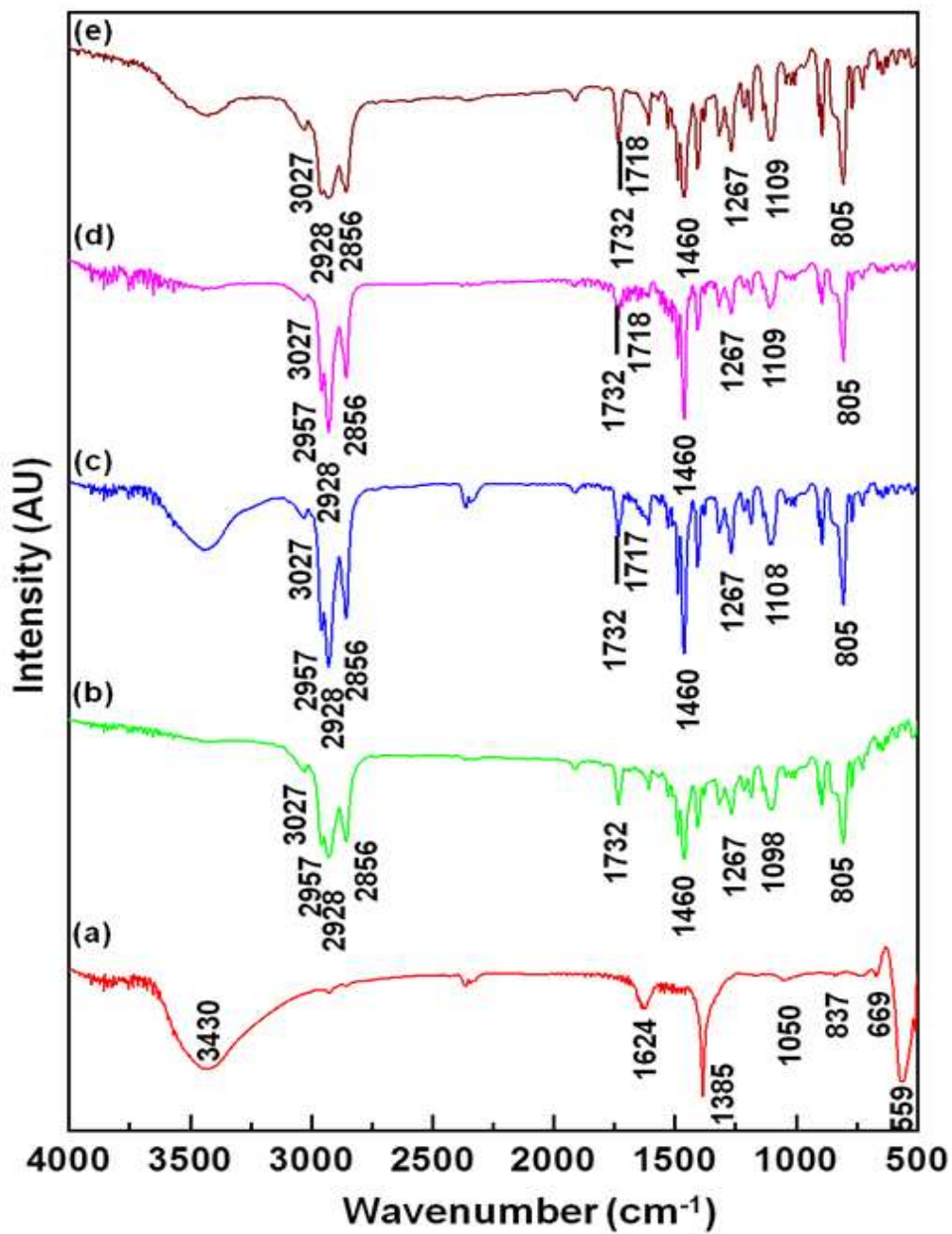


Figure 1. FTIR spectra of the (a) CeO₂ NPs, (b) KCLFC 10s, (c) 1 μ l, (d) 3 μ l and (e) 5 μ l CeO₂ NPs dispersed KCLFC 10s

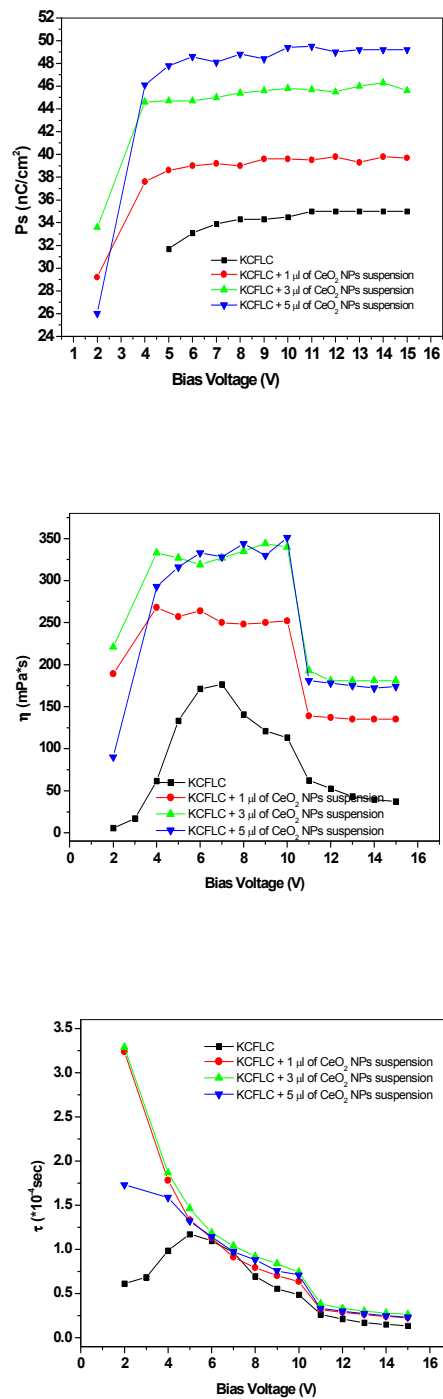


Figure 2. Behavior of (a) spontaneous polarization (P_s), (b) rotational viscosity (η), and (c) response time (τ) of pure KCFLC and np-CeO₂:FLC nanocomposites with applied voltage at 30 °C temperature

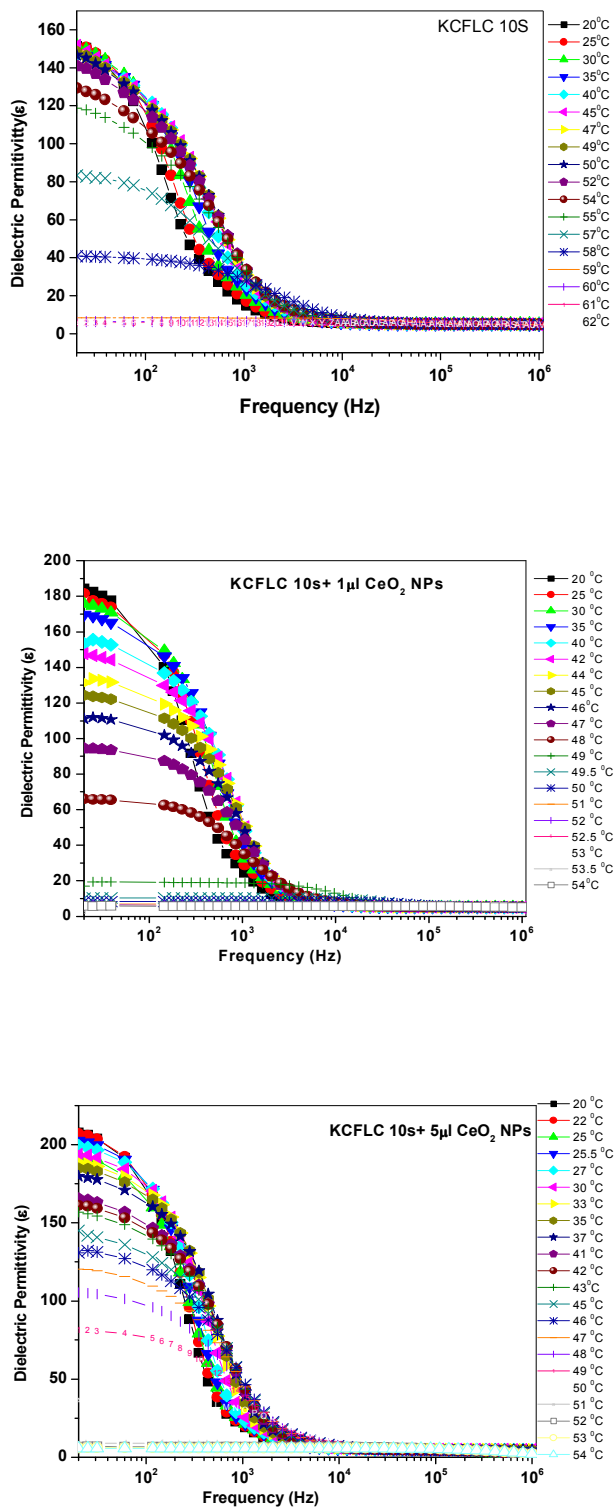


Figure 3. Frequency variation of dielectric permittivity (ϵ') in (a) FLC and (b) 1 μl , (a) 5 μl np-CeO₂:FLC nanocomposites in SmC* -SmA* phase

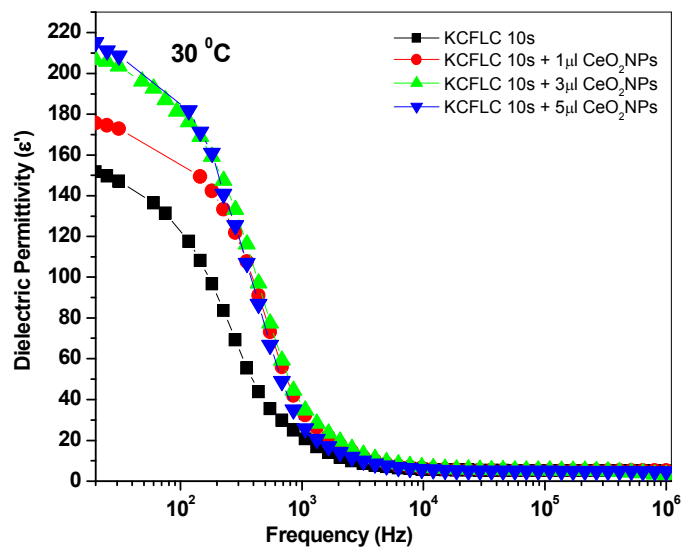


Figure 4. Frequency variation of dielectric permittivity (ϵ') in np-CeO₂ NPs: FLC nanocomposites at 30 °C temperature

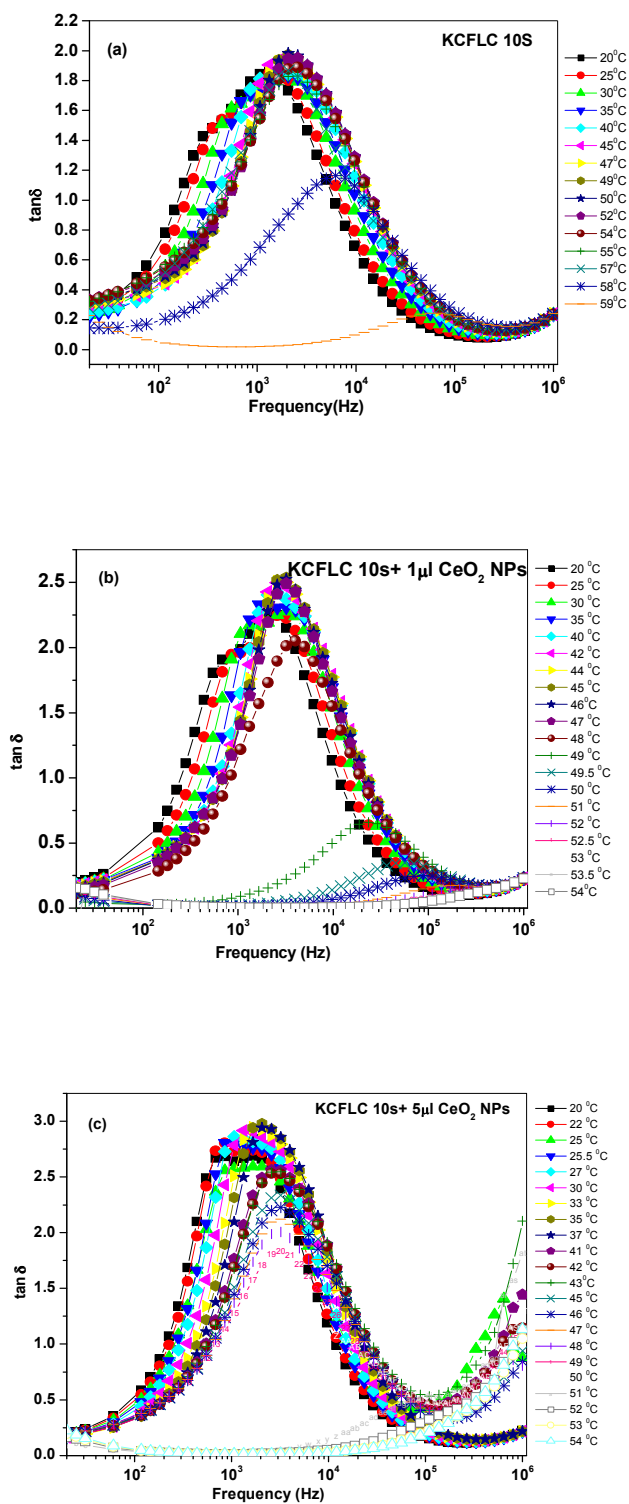


Figure 5. Frequency variation of dielectric losses ($\tan \delta$) in SmC^* - SmA^* phase in (a) FLC and (b) 1 μl , (c) 5 μl np-CeO₂:FLC nanocomposites

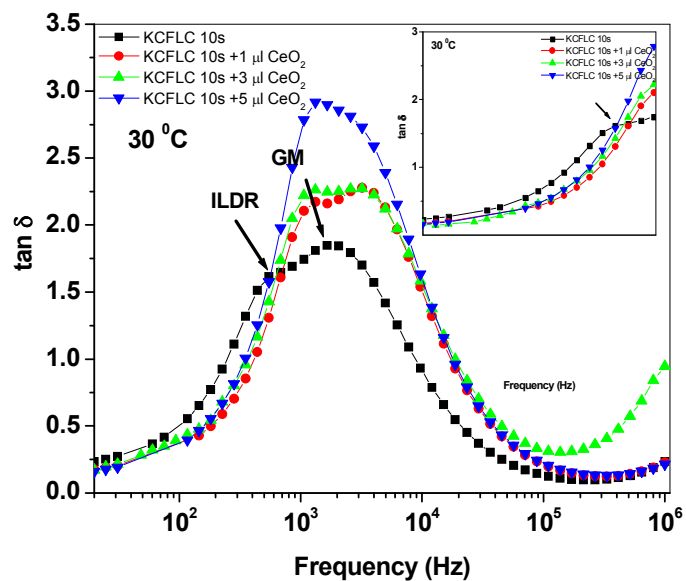


Figure 6. Freq. vs. $\tan \delta$ profile of np-CeO₂:FLC nanocomposites at 30 °C temperature (ILDR- impurity linked dielectric relaxation; GM-Goldstone Mode)